Experimental Neurology 266 (2015) 30–41

Contents lists available at ScienceDirect

Experimental Neurology

journal homepage: www.elsevier.com/locate/yexnr

Regular Article

Experimental optic neuritis induced by the microinjection of lipopolysaccharide into the optic nerve

Marcos L. Aranda, Damián Dorfman, Pablo H. Sande, Ruth E. Rosenstein *

Laboratorio de Neuroquímica Retiniana y Oftalmología Experimental, Departamento de Bioquímica Humana, Facultad de Medicina/CEFyBO, Universidad de Buenos Aires/CONICET, Paraguay 2155, Buenos Aires, Argentina

ARTICLE INFO

Article history:
Received 4 September 2014
Revised 26 December 2014
Accepted 29 January 2015
Available online 14 February 2015

Keywords:
Optic nerve
Lipopolysaccharide
Optic neuritis
Visual evoked potentials
Pupil light reflex
Inflammation
Demyelination
Neurodegeneration

ABSTRACT

Optic neuritis (ON) is a condition involving primary inflammation, demyelination, and axonal injury in the optic nerve which leads to retinal ganglion cell (RGC) loss, and visual dysfunction. We investigated the ability of a single microinjection of bacterial lipopolysaccharide (LPS) directly into the optic nerve to induce functional and structural alterations compatible with ON. For this purpose, optic nerves from male *Wistar* rats remained intact or were injected with vehicle or LPS. The effect of LPS was evaluated at several time points post-injection in terms of: i) visual pathway and retinal function (visual evoked potentials (VEPs) and electroretinograms, (ERGs), respectively), ii) anterograde transport from the retina to its projection areas, iii) consensual pupil light reflex (PLR), iv) optic nerve histology, v) microglia/macrophage reactivity (by Iba-1- and ED1-immunostaining), vi) astrocyte reactivity (by glial fibrillary acid protein-immunostaining), vii) axon number (by toluidine blue staining), vii) demyelination (by myelin basic protein immunoreactivity and luxol fast blue staining), viii) optic nerve ultrastructure, and ix) RGC number (by Brn3a immunoreactivity). LPS induced a significant and persistent decrease in VEP amplitude and PLR, without changes in the ERG. In addition, LPS induced a deficit in anterograde transport, and an early inflammatory response consisting in an increased cellularity, and Iba-1 and ED1-immunoreactivity in the optic nerve, which were followed by changes in axonal density, astrocytosis, demyelination, and axon and RGC loss. These results suggest that the microinjection of LPS into the optic nerve may serve as a new experimental model of primary ON.

Introduction

Optic neuritis (ON), the most common optic neuropathy affecting young adults, is a condition involving primary inflammation, demyelination, and axonal injury in the optic nerve which leads to retinal ganglion cell (RGC) loss and visual dysfunction (reviewed by Toosy et al., 2014). Typically, ON affects young adults ranging from 18 to 45 years of age, and also children as young as 4 years (Wilejto et al., 2006). The annual incidence of ON is approximately 5 in 100,000, with a prevalence estimated to be 115 in 100,000 (Martínez-Lapiscina et al., 2014). Clinical features of ON include peri- or retro-ocular pain accentuated by eye movement, abnormal visual acuity and field, reduced color vision, a relative afferent pupillary defect, and abnormal visual evoked potentials (VEPs) (Hickman et al., 2002; Toosy et al., 2014). The funduscopy may appear normal or demonstrate edema of the optic nerve head (papillitis) (Costello, 2013; Kaufman et al., 2000). The visual deficit of ON may worsen over 1 to 2 weeks, and usually begins improving over the next months. However, although the majority of patients recover after several weeks, in ~40% of these patients, vision loss remains permanent (Beck et al., 1992; Horstmann et al., 2013). In addition, even if visual acuity fully improves, most patients have some residual visual function deficits such as disturbances of visual acuity, contrast sensitivity, color vision, visual field, stereopsis, pupillary reaction, and VEPs (Kupersmith et al., 1983; Kaufman et al., 2000). Some studies indicate that the loss of vision after an episode of ON correlates with retinal ganglion cell (RGC) death (Costello et al., 2006; Trip et al., 2005).

ON has many causes; it may be associated to a range of autoimmune or infectious diseases (Horwitz et al., 2014), and it is closely linked to multiple sclerosis (MS). In fact, ON is the initial symptom of MS in 25% of cases and may occur during the disease in about 70%, usually in the relapsing-remitting phase (Toosy et al., 2014). In addition, a broad range of conditions can give rise to or mimic ON. Several infectious and systemic diseases such as sarcoidosis (Constantino et al., 2000), systemic lupus erythematosus (Frigui et al., 2011), and inflammatory bowel disease (Felekis et al., 2009), as well as HIV (Kallenbach and Frederiksen, 2008), and Lyme disease (Blanc et al., 2010), among others, (Eggenberger, 2001; Hickman et al., 2002) have been reported to cause ON. On the other hand, acute ON often occurs as an isolated clinical event without contributory systemic abnormalities, and it is

* Corresponding author at: Departamento de Bioquímica Humana, Facultad de Medicina/CEFyBO, Universidad de Buenos Aires/CONICET, Paraguay 2155, 5P, (1121), Buenos Aires, Argentina. Fax: +54 11 4508 3672x31.
E-mail address: ruthr@fmed.uba.ar (R.E. Rosenstein).

http://dx.doi.org/10.1016/j.expneurol.2015.01.010
0014-4886/

retrospectively diagnosed as idiopathic (or primary) ON (Optic Neuritis Study Group, 2008; Hickman et al., 2002). Based on the clinical association between MS and ON, the most commonly used experimental model for ON studies is experimental autoimmune encephalomyelitis (EAE), an established model of human MS, which involves an immune-mediated demyelination process. EAE-ON can be induced by immunization with different myelin antigens, such as myelin basic protein (MBP), proteolipid protein (PLP), and myelin oligodendrocyte glycoprotein (MOG) (Furlan et al., 2009; Simmons et al., 2013; Rangachari and Kuchroo, 2013). In fact, when it is associated with MS, ON occurs as an inflammatory demyelinating disorder of the optic nerve (Toosy et al., 2014). However, since the optic nerve lesions in EAE are always associated with inflammation and demyelination of the brain and spinal cord, this model does not mimic the primary form of ON. Moreover, the optic nerve damage in EAE is relatively unpredictable, with different animals developing varying severities of ON (Bettelli et al., 2003; Shindler et al., 2006). Experimental ON was also induced by the injection of lysolecithin, a major component of oxidized low-density lipoproteins, which has a detergent effect on myelin and myelinating cells. Lysolecithin has been successfully used to induce optic nerve demyelination in primates and rats (Lachapelle et al., 2005; You et al., 2011). However, although the lysolecithin model reproduces the focal demyelination in the optic nerve, this ON model lacks the primary inflammatory component, which is a characteristic of human ON. Experimentally, inflammation can be induced in most tissues by the local injection of bacterial lipopolysaccharide (LPS). LPS affects microglia and astrocytes (reviewed by Cunningham, 2013), and produces the activation of glial cells *in vivo* after its intracerebral injection (Bourdiol et al., 1991; Herrera et al., 2000). Moreover, a substantial demyelination resulting from the focal inflammatory lesion caused by the injection of LPS directly into the rat dorsal funiculus was demonstrated (Felts et al., 2005). However, the effect of LPS injection directly into the optic nerve has not been previously examined. Therefore, we considered it worthwhile to analyze the consequences of directly injecting LPS into the optic nerve in order to develop an experimental model of primary ON.

Materials and methods

Animals

Male *Wistar* rats (300 ± 50 g) were housed in a standard animal room with food and water *ad libitum* under controlled conditions of temperature (21 ± 2 °C), luminosity (200 lx), and humidity, under a 12-hour light/12-hour dark lighting schedule (lights on at 8:00 AM). All animal procedures were in strict accordance with the ARVO Statement for the Use of Animals in Ophthalmic and Vision Research. The ethic committee of the School of Medicine, University of Buenos Aires (Institutional Committee for the Care and Use of Laboratory Animals, (CICUAL)) approved this study, and all efforts were made to minimize animal suffering.

Microinjection of LPS

Animals were anesthetized with ketamine hydrochloride (150 mg/kg) and xylazine hydrochloride (2 mg/kg) administered intraperitoneally. Animal's head was shaved and the skin was disinfected with povidone-iodine (Pervinox). A lateral canthotomy was made to perform an incision of 2–3 mm. Lacrimal glands and extraocular muscles were dissected to expose 3 mm of the retrobulbar optic nerve under a surgical microscope. The optic nerve sheaths were opened longitudinally and a microinjection was performed with a 30G needle attached to a Hamilton syringe (Hamilton, Reno, NV, USA). The needle was inserted into the optic nerve as superficially as possible, 2 mm posterior to the globe, and 1 μl of 4.5 μg/μl *Salmonella typhimurium* LPS (Sigma Chemical Co., St Louis, MO, USA) in pyrogen-free saline, was injected for approximately 10 s. In some experiments, the contralateral optic nerves were injected with the same volume of vehicle (pyrogen free saline), whereas in another set of experiments, animals were injected with vehicle or LPS in one optic nerve, while the contralateral optic nerve remained intact. After the injection, the skin incision was sutured and antibiotics were topically administered to prevent infection.

Visual evoked potential recording

Animals were anesthetized as described above. Under stereotaxic control, two stainless steel electrodes, used as positive electrodes, were surgically placed 3 mm lateral to the inter-hemispheric suture and 5.6 mm behind bregma penetrating the cortex to approximately 0.5 mm. Reference electrodes were placed 2 mm lateral to the midline and 2 mm anterior to the bregma, as previously described (Belforte et al., 2011). The electrodes were isolated and covered with dental acrylic; skin was sutured with nylon 5/0, and antibiotics were administered topically.

After 5 days of electrode implantation, animals were dark adapted for 6 h, and anesthetized as described before. All recordings were made within 20 min after injection of anesthetic. The pupils were dilated with proparacaine (Alcon Midryl, Alcon Laboratories, Buenos Aires, Argentina), and the cornea was intermittently irrigated with saline. Each eye was individually recorded, occluding the contralateral eye with black carbon paper and cotton, and an average of 70 stimuli was recorded. Eyes were stimulated with unattenuated white light (1 Hz) by a photostimulator with an intensity of 5 cd s/m^2, with filters for low and high frequencies (0.5 to 100 Hz, respectively) and a 12.5 mV gain. The amplitude and latency of P1–N1 and N1–P2 components of VEPs were assessed with software Akonic Bio-PC (Akonic, Buenos Aires, Argentina) coupled to a PC.

Electroretinography

Electroretinograms (ERGs) were recorded as previously described (Dorfman et al., 2013). Briefly, rats were dark-adapted for 6 h, and anesthetized under dim red illumination. Pupils were dilated by topical application of phenylephrine hydrochloride and tropicamide (Anestalcon, Alcon Laboratories, Buenos Aires, Argentina), and the cornea was intermittently irrigated with saline solution. Rats were placed facing the stimulus at a distance of 20 cm. A reference electrode was placed through the ear, a gold electrode was placed in contact with the central cornea and a grounding electrode was attached to the tail. Scotopic ERGs were recorded from both eyes simultaneously and 15 responses to flashes of unattenuated white light (5 ms, 0.2 Hz) from a full-field/Ganzfeld stimulator (light-emitting diodes) set at maximum brightness (5 cd s/m^2 without filter) were amplified, filtered (1.5-Hz low-pass filter, 1000 high-pass filter, notch activated) and averaged (Akonic BIO-PC, Buenos Aires, Argentina). The a-wave and b-wave amplitude and latency were measured as previously described (Dorfman et al., 2013).

Cholera toxin β-subunit transport studies

At 4 days post-injection of vehicle or LPS, rats were anesthetized, and a drop of 0.5% proparacaine (Anestalcon, Alcon Laboratories, Buenos Aires, Argentina) was topically administered for local anesthesia. Using a 30G Hamilton syringe (Hamilton, Reno, NV, USA), 4 μl of 0.1% cholera toxin β-subunit (CTB) conjugated to Alexa 488 dye (Molecular Probes Inc., Eugene, OR, USA) in 0.1 mol/l PBS (pH 7.4) was injected into the vitreous, as previously described (Dorfman et al., 2013). The injections were applied 1 mm from the limbus, and the needle was left in the eye for 30 s to prevent volume loss. Three days after injection, rats were anesthetized and intracardially perfused. Brains were carefully removed, post-fixed overnight at 4 °C, and immersed in a graded series of sucrose solutions for cryoprotection; coronal sections (40 μm) were obtained using a freezing microtome (CM 1850, Leica, Leica Microsystems,

Buenos Aires, Argentina), mounted in glasses and viewed under an epifluorescence microscope (BX50, Olympus, Duarte, CA, USA).

Pupillary light reflex

Animals were injected with vehicle or LPS in one optic nerve while the contralateral optic nerve remained intact. The animals were dark-adapted for 2 h. In some experiments, the eye in which the nerve was injected with vehicle or LPS was stimulated with high intensity light (1200 lx) for 30 s and pupil light reflex (PRL) was recorded in the contralateral (intact) eye. In another set of experiments, the light stimulus was applied into the intact eye, and the contraction of the pupil of the contralateral eye (injected with vehicle or LPS) was recorded. The recordings were made under infrared light with a digital video camera (Sony DCR-SR60, Tokyo, Japan), as previously described (Fernandez et al., 2013). The sampling rate was 30 frames per second. Images were acquired with OSS Video Decompiler Software (One Stop Soft, New England, USA). The results were expressed as the percentage of the pupil contraction before (steady state) and 30 s after the light pulse.

Histological evaluation

Animals were deeply anesthetized and intracardially perfused with saline, followed by a fixative solution (4% paraformaldehyde in phosphate buffer (PBS), pH 7.2). Optic nerves were obtained from the optic nerve head to the optic chiasm and post-fixed in fixative solution for 24 h at 4 °C. After several washes, the samples were dehydrated, cleared in butyl-acetate and embedded in paraffin. Serial longitudinal and transversal sections (5 μm) were obtained using a microtome (Leica, Leica Microsystems, Buenos Aires, Argentina). Some sections were used for histological analysis (hematoxylin-eosin (H&E) staining). The total transverse area and the number of nuclei per section were measured. Measurements (×400) were obtained at 1 mm dorsal and ventral from the optic disk. The average thickness (in μm) of the total retina, inner plexiform layer (IPL), inner nuclear layer (INL), outer plexiform layer (OPL), outer nuclear layer (ONL), and photoreceptor outer segments (OS) were measured. For each sample, the average of four different sections was used as the representative value. After deparaffinization, some sections were hydrated and immersed overnight at 60 °C in 0.1% luxol fast blue (Biopack, Buenos Aires, Argentina) in acidified 95% ethanol. Differentiation and counterstaining were carried out with 0.01% Li_2CO_3 and incubation for 5 min in 0.5% neutral red (Biopack, Buenos Aires, Argentina). Sections were mounted and viewed under an optic microscope (Nikon Eclipse E400, Tokyo, Japan). Light microscopic images (200× and 1000×) were digitally captured *via* a Nikon Coolpix S10 camera (Nikon, Tokyo, Japan).

Semi-thin section processing

Anesthetized rats were intracardially perfused with saline solution, followed by a fixative solution containing 4% formaldehyde and 2% glutaraldehyde in 0.1 mol/l PBS (pH 7.4). Optic nerves were carefully removed, and portions (2 mm) near the eye were obtained and embedded in the same fixative solution for 24 h. After several washings, some tissue blocks were post-fixed in 2% aqueous osmium tetroxide in sodium phosphate buffer, for 1 h. Dehydration was accomplished by gradual ethanol series, and tissue samples were embedded in epoxy resin. Semi-thin sections (0.5 μm) obtained with an ultramicrotome (Ultracut E, Reichert-Jung, Austria) were stained with toluidine blue, and used for morphometric analysis. Light microscopic images (1000×) were digitally captured using a Nikon Eclipse E400 microscope *via* a Nikon Coolpix S10 camera (Nikon, Tokyo, Japan). Images obtained were assembled and processed using Adobe Photoshop CS5 (Adobe Systems, San Jose, CA, USA) to adjust brightness and contrast. Analysis image software (Image J, National Institutes of Health, Bethesda, Maryland;http://imagej.nih.gov/ij/) were used to determinate axonal density and axon number.

Immunohistochemical studies

Antigen retrieval was performed by heating slices at 90 °C for 30 min in citrate buffer (pH 6.3). The following antibodies were used: a goat anti-ionized calcium binding adaptor molecule 1 (Iba-1) antibody (1:500; Abcam Inc., Buenos Aires, Argentina), a mouse anti-ED1 antibody (1:500; Abcam Inc., Buenos Aires, Argentina), a mouse monoclonal anti-glial fibrillary acidic protein (GFAP) antibody conjugated to Cy3 (1:1200; Sigma Chemical Co., St Louis, MO, USA), a donkey anti-mouse secondary antibody conjugated to Alexa 488 (1:500; Molecular Probes, Buenos Aires, Argentina), a rabbit polyclonal anti-MBP antibody (1:1000, kindly supplied by Dr. Campagnoni, Mental Retardation Research Center, University of California, Los Angeles, CA, USA), a goat anti-mouse and a donkey anti-rabitt secondary antibodies conjugated to Alexa 568 (1:500; Molecular Probes, Buenos Aires, Argentina). Sections were immersed in 0.1% Triton X-100 in 0.1 mol/l PBS for 10 min, incubated with 2% normal horse serum for 1 h for unspecific blockade, and then incubated overnight at 4 °C with the primary antibodies. After several washings, secondary antibodies were added, and sections were incubated for 2 h at room temperature. Regularly, some sections were treated without the primary antibodies to confirm specificity. For each nerve, results obtained from four separate regions were averaged, and the mean of 5 nerves was recorded as the representative value for each group. For immunodetection of RGCs, retinas were carefully detached and flat-mounted with the vitreous side up in superfrost microscope slides (Erie Scientific Company, Portsmouth, New Hampshire, USA). Whole-mount retinas were incubated overnight at 4 °C with a goat anti-Brn3a antibody (1:500; Santa Cruz Biotechnology, Buenos Aires, Argentina). After several washes, a donkey anti-goat secondary antibody conjugated to Alexa 568 (1:500; Molecular Probes, Buenos Aires, Argentina) was added, and incubated for 2 h at room temperature. Finally, retinas were mounted with fluorescent mounting medium, (Dako, Glostrup, Denmark), and observed under an epifluorescence microscope (BX50; Olympus, Tokyo, Japan) connected to a video camera (3CCD; Sony, Tokyo, Japan), attached to a computer running image analysis software (Image-Pro Plus; Media Cybernetics Inc., Bethesda, MD, USA). For each retina, results obtained from eight separate quadrants (four from the center and four from the periphery) were averaged, and the mean of 5 eyes was recorded as the representative value, as previously described. Immunofluorescence studies were performed by analyzing comparative digital images from different samples by using identical exposure time, brightness, and contrast settings.

Electron microscopy

Animals were intracardially perfused with a fixative solution, containing 2% glutaraldehyde and 4% formaldehyde in 0.1 mol/l PBS (pH 7.4). Optic nerves were obtained as previously described, and ultrathin sections (70 nm) were obtained using glass knives and an ultramicrotome Ultracut E (Reichert-Jung, Austria). Sections were mounted on 200 *Mesh* grids and stained with uranyl acetate (2% in 70% ethanol) and Reynolds lead citrate. Finally, sections were viewed and photographed using a Zeiss 109T transmission electron microscope (Carl Zeiss Microscopy, Peabody, MA, USA), equipped with a digital camera (ES1000W, Gatan, Pleasanton, CA, USA).

Morphometric analysis

All the images obtained were assembled and processed using Adobe Photoshop CS5 (Adobe Systems, San Jose, CA, USA) to adjust brightness and contrast. No other adjustments were made. For all morphometric image processing and analysis, digitalized captured TIFF images were

transferred to ImageJ software (National Institutes of Health, Bethesda, Maryland;http://imagej.nih.gov/ij/).

Peripheral white blood cell and cerebrospinal fluid cell number

Peripheral white blood cell and cerebrospinal fluid cell number were assessed at 2 days post-injection in rats in which one optic nerve was injected with LPS and in animals whose optic nerves remained intact, by use of a Neubauer camera and light microscopy. The technique for collecting cerebrospinal fluid from the cisterna magna was performed according to Consiglio and Lucion (2000).

Body temperature assessment

For body temperature measurements, a rectal probe was inserted 2 cm into the rectum, as previously described (Salido et al., 2013).

Statistical analysis

Data are presented as mean ± standard error (SE). Statistical analysis of results was performed by Student's *t*-test or two-way analysis of variance (ANOVA), followed by Tukey's test. *P* values below 0.05 were considered statistically significant.

Results

Functional studies

In order to assess the effect of LPS injected into the optic nerve on the visual pathway function, flash VEPs were recorded at different time points after microinjections. Fig. 1 depicts the average amplitude of VEP P1–N1 and N1–P2 components, registered in animals in which one optic nerve remained intact (control), and the contralateral optic nerve was injected with vehicle or LPS. LPS induced a decrease in VEP P1–N1 and N1–P2 component amplitude, which was significant from day 1 and 4 post-injection, respectively, as compared with intact or vehicle-injected optic nerves. No further decrease in these parameters was observed until 21 days post-injection of LPS. No significant differences in P1, N1, and P2 latency were observed among groups, and no differences in VEP amplitudes and latencies were evident between intact and vehicle-injected optic nerves along the study. Representative waveforms of VEPs from all the experimental groups at days 1 and 21 post-injection are also shown in Fig. 1. No significant differences in the average amplitude and latency of scotopic ERG a- and b-waves were observed among groups, until day 21 post-injection (Supplementary Fig. 1).

The active anterograde transport from RGCs to the SC was analyzed using CTB intravitreally administered in animals in which one optic nerve was injected with vehicle and the contralateral optic nerve was injected with LPS. At 7 days after injections, CTB labeled the entire retinotopic projection to the most superficial layers (*i.e.* the *stratum zonale* and the *stratum griseum superficiale*) of the SC contralateral to optic nerves injected with vehicle, whereas a clear reduction in CTB staining was observed in the central and lateral regions of the SC contralateral to optic nerves injected with LPS (Fig. 2). A similar effect of LPS on CTB staining pattern was observed in the LGN and OPN, as also shown in Fig. 2.

In order to further analyze the functional consequences of LPS injection into the optic nerve, the PLR was examined in animals in which one optic nerve was injected with vehicle or LPS, while in both cases, the

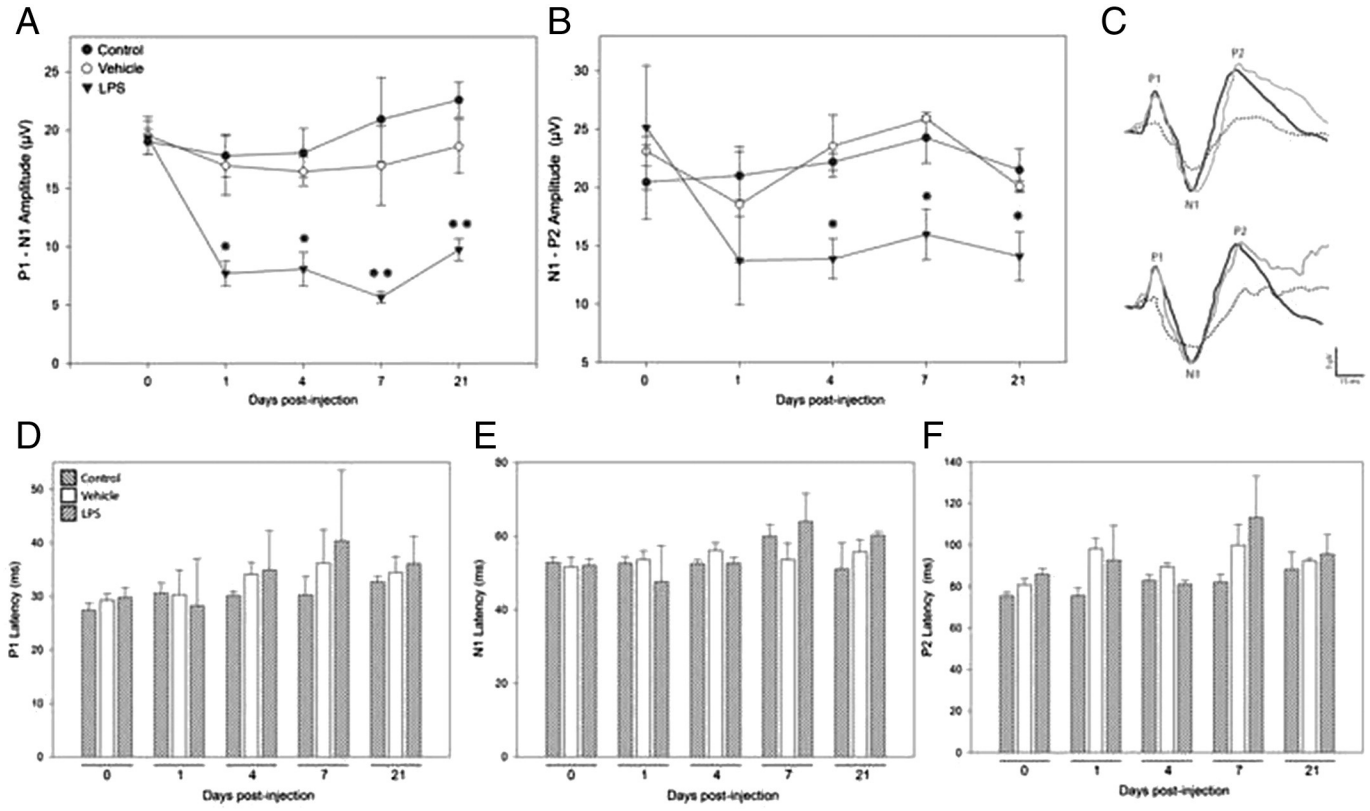

Fig. 1. Effect of LPS on VEPs. Panel A: average amplitudes of VEP P1–N1 component. Panel B: average amplitudes of VEP N1–P2 component. Optic nerves remained intact (black circles) or were injected with vehicle (white circles) or LPS (black triangles), and VEPs were recorded at different time points post-treatment. As compared with intact or vehicle-injected optic nerves, LPS induced a decrease in VEP P1–N1 and N1–P2 component amplitude which was significant from day 1 (panel A), and day 4 (panel B), respectively. Data are mean ± SEM (n: 10 optic nerves/group). $^{*}P < 0.05$, $^{**}P < 0.01$ *vs.* intact or vehicle-injected optic nerves, by Tukey's test. Panel C: representative VEP traces from an intact optic nerve (black line), vehicle-injected optic nerve (gray line), or LPS injected optic nerve (dotted line) at 1 (upper traces) and 21 days (lower traces) post-injections. P1, N1, and P2 latencies are shown in panels D, E, and F, respectively. No significant differences in VEP latencies were observed among groups along the study.

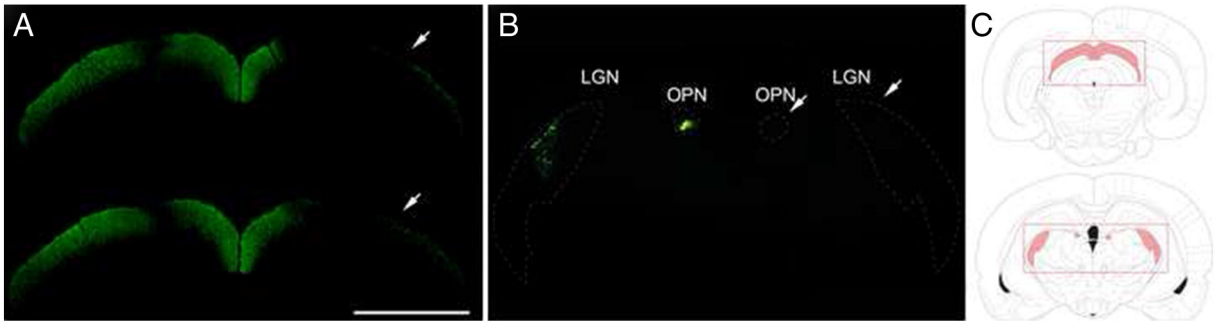

Fig. 2. Effect of LPS injection on CTB-staining pattern in the SC, LGN, and OPN. Panel A: Representative photomicrographs of coronal sections of the SC from an animal in which one optic nerve was injected with vehicle, and the contralateral optic nerve was injected with LPS. A clear reduction of the retinal terminal field density in the SC contralateral to the LPS-injected optic nerve was observed (arrow), as compared with the SC contralateral to an optic nerve injected with vehicle. Panel B: A similar pattern of alterations in CTB-staining was observed in the LGN and OPN contralateral to optic nerves injected with LPS (arrow). Shown are photomicrographs representative of 5 animals. Scale bar = 1 mm. Panel C: The analyzed zones are represented in red.

contralateral optic nerve remained intact. When light stimulated eyes in which the optic nerve was injected with LPS, a significant decrease in the magnitude of pupil contraction of the contralateral intact eye was observed at all time points examined, as shown in Fig. 3. No differences in PRL were observed in vehicle-injected nerves along the study (data not shown). When light stimulated the intact eye, no differences in pupil constriction were observed between both groups at all time points post-injection (Supplementary Fig. 2).

Structural and ultrastructural studies of the optic nerve

To assess structural changes, optic nerve longitudinal and transversal sections were stained with H&E (Fig. 4). A significant increase in nucleus number was detected in LPS-injected optic nerves as early as 1 day, and persisted until 21 days post-injection, as compared with vehicle-injected optic nerves. The quantitation of nuclei in the optic nerve indicated a significant increase in this parameter at all time points post-injection of LPS. In addition, LPS induced a significant increase in optic nerve cross-section area at 7 and 21 days post-injection. No differences in nucleus number and optic nerve cross-section areas were detected at different time point post-injection of vehicle into the optic nerve, and between intact and vehicle-injected optic nerves along the study (data not shown).

Microglia/macrophages were analyzed by Iba-1 and ED1 immunostaining, as shown in Fig. 5. An increase in Iba-1 and ED1 immunoreactivity was observed in optic nerves injected with LPS. Measurement of the Iba-1(+) area revealed a significant increase in this parameter at 1 day after LPS injection, while from day 4 post-injection, the Iba-1(+) area was significantly higher than at 1 day post-injection and remained unchanged until day 21. In vehicle-injected optic nerves, and at 1 day post-injection of LPS, ED1 immunoreactivity was undetectable, while an increase in this parameter was observed at 4 and 7 days post-injection, which was lower at 21 days post-LPS. In addition, a significant increase in GFAP(+) area was evident at 21 days post-injection of LPS (Fig. 5). No differences in Iba-1, ED1, and GFAP immunostaining were observed at different time points post-injection of vehicle, and between control and vehicle-injected optic nerves (data not shown).

Optic nerve axons were analyzed by toluidine blue staining. In cross-sectioned optic nerve injected with LPS, a significant decrease in axonal density was observed at 7 days post-injection, and a decrease in axon number was evident at 21 days after LPS injection, as shown in Fig. 6. Fig. 7 shows an analysis of MBP (a reliable index of oligodendrocyte

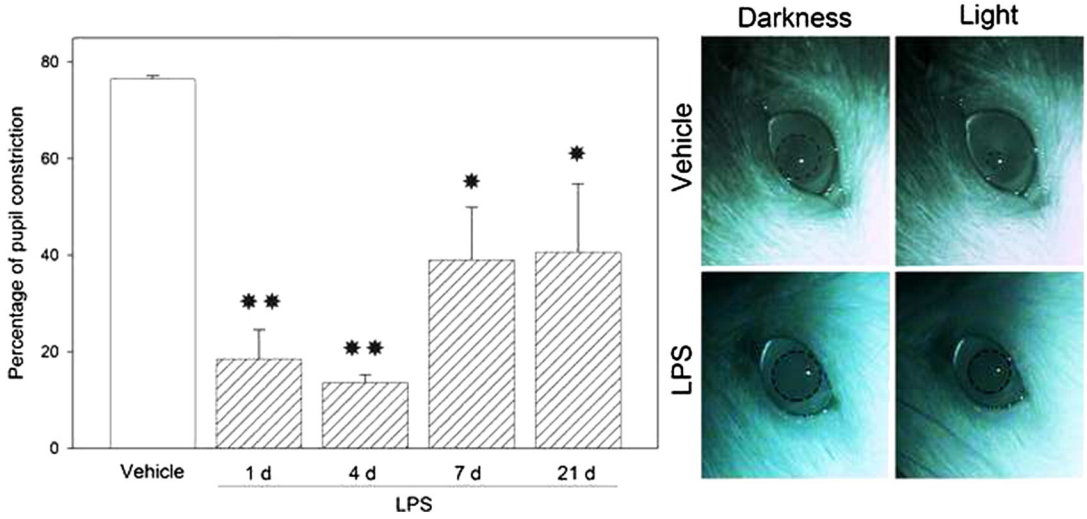

Fig. 3. Effect of LPS on consensual PLR. Left: The pupil diameter (relative to the limbus diameter) was measured at different time points after vehicle or LPS injection into the optic nerve, and the percentage of pupil constriction was calculated in the contralateral eye whose optic nerve remained intact. The average of pupillary constriction in response to a light flash (1200 lx) significantly decreased at the first day after LPS injection into the optic nerve and remained reduced until 21 days post-injection. Data are the mean ± SEM (n = 8 eyes/group). $^{*}P < 0.05$, $^{**}P < 0.01$ *vs.* vehicle, by Tukey's test. Right: Representative images of the consensual PRL in an animal in which one optic nerve was injected with vehicle or LPS, at 1 day post-injection.

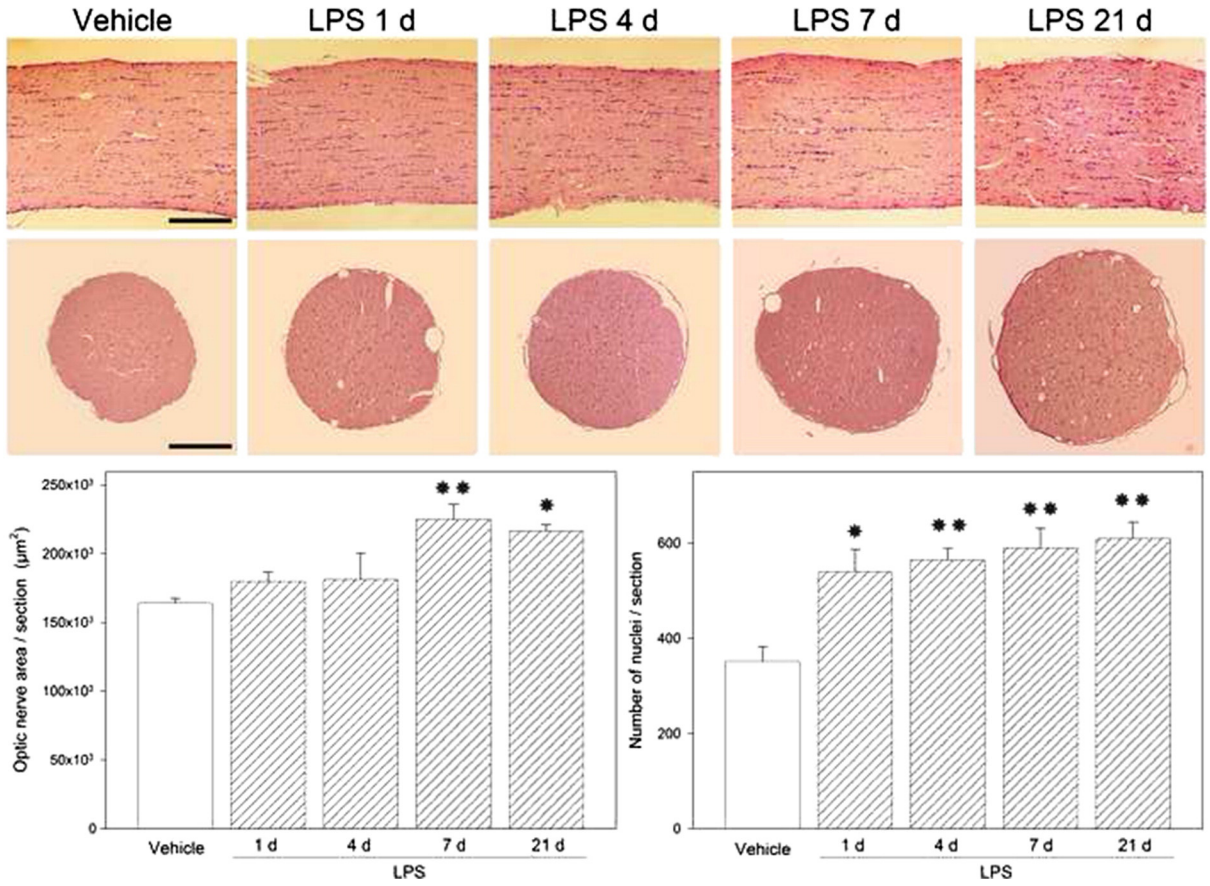

Fig. 4. Effect of LPS on the optic nerve structure. Shown are representative optic nerve longitudinal (upper panel) and cross-sections (medium panel) at 21 days post-injection of vehicle and at 1, 4, 7, and 21 days post-injection of LPS, stained with H&E. The ends proximal to the globes are on the left, and the ends distal to the globes are on the right. An increase in nucleus number was detected in LPS-injected optic nerves as early as 1 day and persisted until 21 days post-injection, as compared with vehicle-injected optic nerves. Note the increased cross-section area in LPS-injected optic nerve at 7 and 21 days post-injection. Lower panel: quantification of optic nerve cross-section area, and number of nuclei/section. The injection of LPS significantly increased the optic nerve cross-section area at 7 and 21 days post-injection, while the increase in the number of nuclei was evident at 1 day and persisted until 21 days post-injection of LPS. Data are the mean ± SEM (n = 5 optic nerves/group). $^{*}P < 0.05$, $^{**}P < 0.01$ *vs.* vehicle-injected optic nerves, by Tukey's test. Scale bar = 200 µm.

differentiation and myelin formation) in cross-sectioned optic nerves. A decrease in MBP-immunoreactivity was observed at 21 days post-injection of LPS, while no changes in MBP-immunostaining were observed at 7 days post-injection. Demyelination was assessed by luxol fast blue staining. Signs of demyelination were evident at 21 (but not 7) days post-injection of LPS (Fig. 8).

At ultrastructural level, myelin was highly disorganized, and frequent lamellar membranous bodies were observed at 21 days post-injection of LPS, while at 7 days, occasional demyelinated axons were observed (Fig. 9). No ultrastructural alterations in vehicle-injected optic nerve along the study, and at 1 and 4 days post-injection of LPS were observed (data not shown).

Retinal studies

The retinal structure from intact, vehicle- or LPS-injected optic nerve was analyzed (Fig. 10). A morphometric analysis of retinal sections performed at 21 days post-injection of LPS, revealed no differences in the total retina, IPL, INL, OPL, ONL, and OS layer thickness. To specifically examine RGCs, Brn3a immunostaining was analyzed in flat-mounted retinas. A significant decrease in the Brn3a(+) cell number was observed at 21 days post-injection of LPS, as shown in Fig. 9. No changes in this parameter were observed in the retina from vehicle-injected optic nerves along the study or at 1, 4, and 7 days post-injection of LPS (data not shown).

Peripheral white blood cell and cerebrospinal fluid cell number, and corporal temperature assessment

At 2 days post-injection, in rats which were injected with LPS into one optic nerve, mean peripheral white blood cell count (8990 ± 840 cells/ml) did not significantly differ from that observed in rats whose optic nerves remained intact (9968 ± 920 cells/ml), (n = 5 animals/group). Moreover, LPS injection did not affect cerebrospinal fluid cell count (*i.e.*, LPS: 12.3 ± 3 cells/µl, control: 10.9 ± 4 cells/µl, n = 5 animals/group), and no significant differences in body temperature were observed between LPS-injected and control rats (*i.e.*, LPS: 37.5 °C ± 0.2 °C, control: 37.5 °C ± 0.3 °C, n = 5 animals/group).

Discussion

For the first time, the present results demonstrate that a single microinjection of LPS directly into the optic nerve induced functional and histological alterations which mimicked central features of primary ON. In the present study, we have analyzed the consequences of LPS injection into the optic nerve during a 21-day period, that could be apportioned to approximately 2 phases: an early phase characterized by functional (VEPs, anterograde transport, PLR) alterations, and microglial/macrophage reactivity in the optic nerve, followed by a late phase at which functional alterations and microglial/macrophage

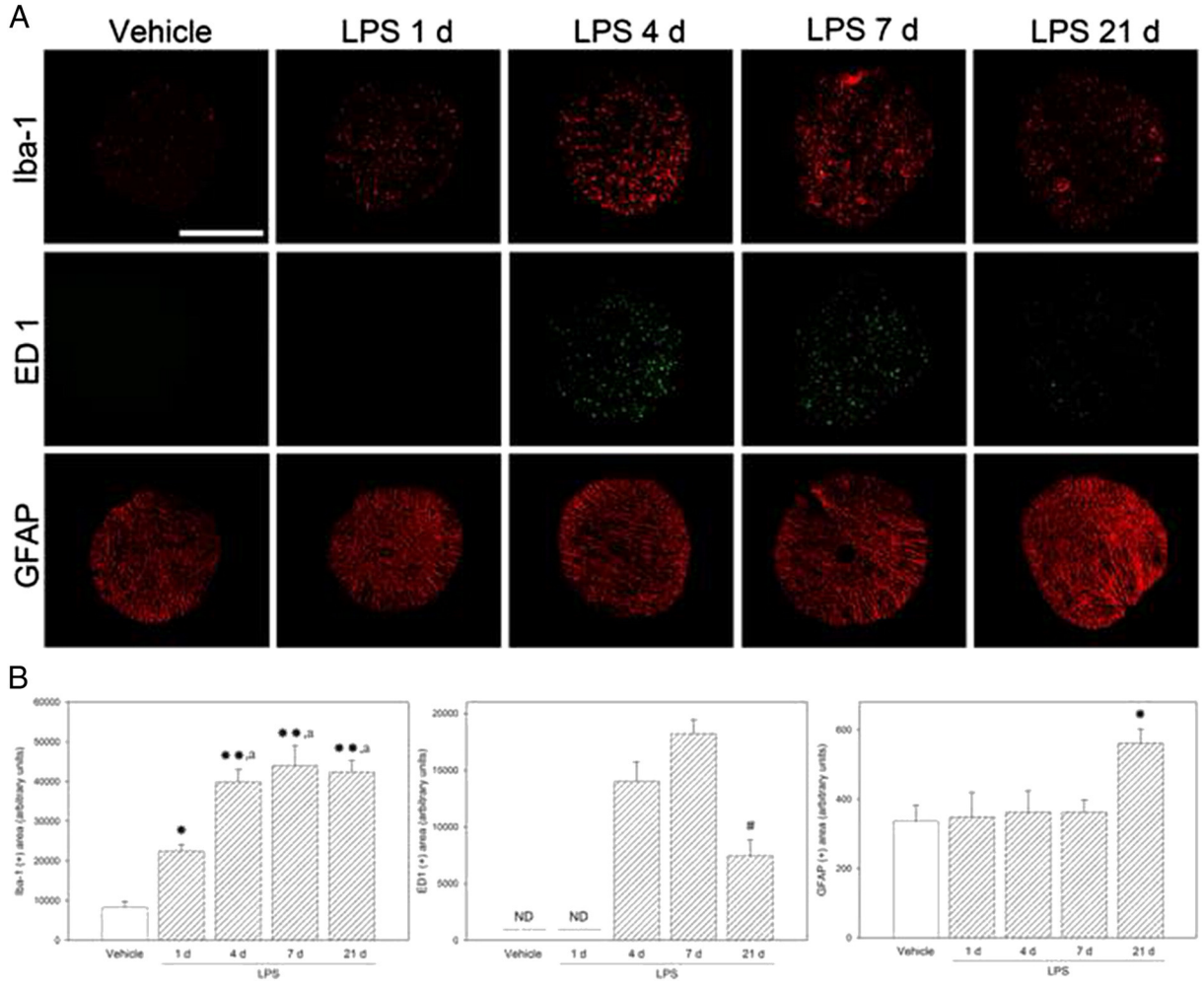

Fig. 5. Microglia/macrophage and astrocyte analysis in the optic nerve. Panel A: Representative photomicrographs showing Iba-1 (upper panel), ED1 (middle panel) and GFAP (lower panel) immunostaining patterns in cross-sections from optic nerves at 21 days post-injection of vehicle and at 1, 4, 7, and 21 days post-injection of LPS. Panel B: Analysis of Iba-1 (+), ED1(+), and GFAP(+) area. The injection of LPS into the optic nerve induced a significant increase of Iba-1(+) area at day 1, and a further increase of this parameter at 4, 7, and 21 days post-injection. ED1 immunoreactivity was undetectable in vehicle-injected optic nerves and in LPS-injected optic nerve at 1 day post-injection, while an increase in this parameter was observed at 4, and 7 days, which was lower at 21 days post-injection. LPS induced GFAP upregulation at 21 days post-injection. Data are the mean ± SEM (n = 5 optic nerves per group); $^{*}P < 0.05$, $^{**}P < 0.01$, *vs.* optic nerves injected with vehicle, a: $P < 0.05$ *vs.* optic nerves injected with LPS at 1 day post-injection, #: $P < 0.05$ *vs.* LPS at 4 or 7 days post-injection, by Tukey's test. Scale bar = 200 μm.

reactivity persisted, and reactive gliosis, demyelination, and axonal and RGC loss were evident. This sequence of alterations differed from the profile observed in autoimmune ON (EAE-NO) models, in which demyelination is a primary event (Zhu et al., 1999). In this sense, although EAE models mimic ON associated with MS, the injection of LPS into the optic nerve could reproduce a form of ON that is characterized by a prominent axonal degeneration with only a mild demyelination.

VEPs reflect the activity of all cells in the pathway from photoreceptors to visual cortex, and as such, are considered a useful noninvasive tool for investigating the visual system function, particularly in ON patients (Kupersmith et al., 1983; Halliday et al., 1972; Hood et al., 2000). As shown herein, LPS provoked a significant and persistent decrease of VEP P1–N1 and N1–P2 amplitude. Since LPS did not affect the flash ERG along the study, the early decrease in VEP amplitude could be attributed to an extra-retinal visual pathway alteration. It is assumed that the VEP amplitude reflects the number of functional optic nerve fibers, while a latency increase is considered an index of optic nerve demyelination (You et al., 2011). The fact that the decrease in VEP component amplitude was already evident at 1 day post-injection of LPS (*i.e.*, before any significant change in axon number) indicates that the functional disturbance predated morphological changes. In ON, the number of functional afferent fibers is influenced by two factors: inflammation severity and axonal degeneration (Klistorner et al., 2008; You et al., 2011). In this way, the early decrease in VEP amplitude induced by LPS injection could reflect the acute inflammatory process in the optic nerve, while axonal atrophy and RGC loss could contribute to the late decrease of this parameter. Contrary to our expectations, no changes in VEP component latency were observed even at 21 days post-injection of LPS, a time point at which demyelination was histologically observed in the optic nerve. In contrast to these results, a decrease in N1 latency was observed in lysolecithin-induced demyelination in rat optic nerves (You et al., 2011), and increased VEP latency was described in EAE-ON models (Diem et al., 2008; Matsunaga et al., 2012). The reasons for this discrepancy are unclear. However, it should be taken into account that in EAE-ON models, demyelination and inflammation distribute widely in the nervous system and therefore, it is difficult to quantify the effect of the optic nerve demyelination itself on signal conduction (You et al., 2011). On the other hand, in the lysolecithin-induced ON, it was shown that the latency prolongation of VEPs corresponds to the size of the demyelinated area in the visual pathway (You et al., 2011). Thus, it seems likely that the size of the demyelinated area in LPS-injected optic nerve could be not enough to influence the myelin integrity of the entire visual pathway.

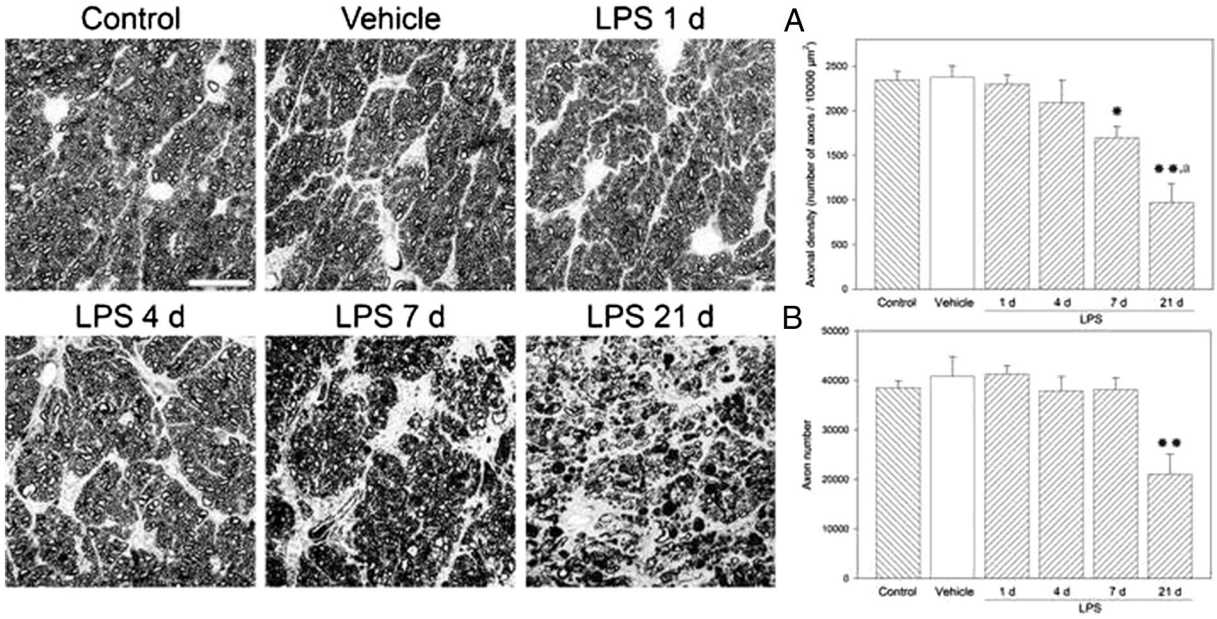

Fig. 6. Effect of LPS on optic nerve axons. Representative images of cross-sections from intact optic nerves, optic nerves at 21 days post-injection of vehicle and at 1, 4, 7, and 21 days post-injection of LPS, stained with toluidine blue. Note the homogeneity of the staining in intact optic nerves, vehicle-injected optic nerves, and LPS-injected optic nerves at 1 and 4 days post-injection. At 7 and 21 days post-injection of LPS, a less stained area were observed. Panel A: assessment of axonal area: LPS induced a significant decrease in axonal density at 7 days which further decreased at 21 days post-injection. Panel B: The injection of LPS into the optic nerve induced a significant decrease in axon number at 21 days post-injection. Data are mean ± SEM (n: 5 optic nerves/group). $^{*}P < 0.05$, $^{**}P < 0.01$ *vs.* intact or vehicle-injected optic nerves, a: $P < 0.05$ *vs.* LPS at 7 days post-injection, by Tukey's test. Scale bar = 25 µm.

In rodents, most RGC axons project contralaterally to the SC, LGN, and OPN (Kondo et al., 1993). The injection of LPS induced a deficit in CTB anterograde transport from the retina to the SC, the LGN and OPN, which supports that LPS induced a "misconnection" between the retina and its projection areas. Recently, a defective axonal transport was described in mice with EAE-ON (Lin et al., 2014). However, in this case, the deficit was attributed to demyelination and axonal injury in the optic nerves, whereas in our experimental setting, the decrease in CTB anterograde transport preceded those structural alterations, supporting that LPS induced an early axonal transport integrity loss, most likely associated to the inflammatory process than to axonal injury and/or demyelination.

The OPN is the primary nucleus in the neural circuit controlling pupil constriction (Gamlin, 2006). Therefore, the significant decrease in afferent PLR induced by LPS is consistent with the decrease in the CTB anterograde transport from the retina to the OPN. In agreement, decreased pupillary responses were described in ON and MS patients (de Seze et al., 2001; Ellis, 1979; Moro et al., 2007). Moreover, consistently with our results, decreased pupillary light responses precede histological evidence of ON in a mouse EAE model (Shindler et al., 2012).

Increased cellularity and cross-sectional area, possibly as a result of edema, were observed at early stages post-injection of LPS. A similar increase in optic nerve cross-section sizes was observed after immunization of Brown Norway rats with MOG (Fairless et al., 2012).

Under normal conditions, microglia surveys the central nervous system (CNS) environment, and promptly responds to injury with process redirection and cell body migration (reviewed by Perry and Teeling, 2013). Moreover, infiltrating macrophages from the peripheral circulation enter the site of injury. Many of the same immunohistochemical markers are expressed in these two cell types which are morphologically indistinguishable from each other; therefore they are often referred to as microglia/macrophages. As shown herein, the injection of LPS induced an early and persistent increase in microglia/macrophage response. In agreement with this result, it was shown that the intranigral injection of LPS on the rat dopaminergic system produces the activation of microglial cells that is already evident 2 days after injection (Herrera

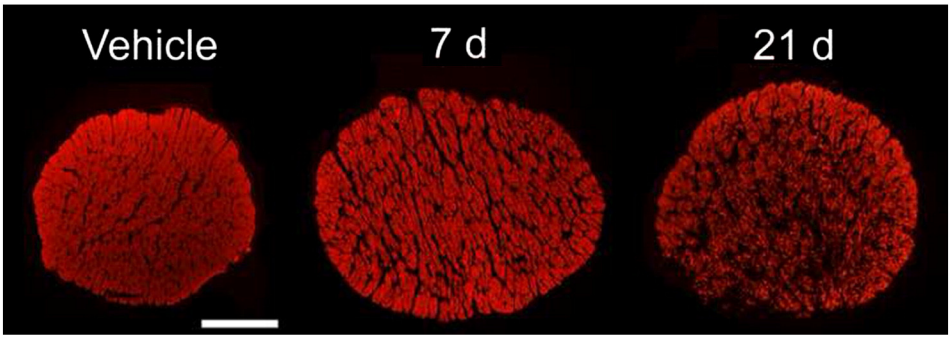

Fig. 7. Effect of LPS on MBP-immunoreactivity. Representative photomicrographs showing MBP immunostaining patterns in cross-sections from optic nerves at 21 days post-injection of vehicle and at 7, and 21 days post-injection of LPS. A decrease in MBP-immunostaining was observed at 21 (but not 7) days post-injection of LPS, as compared with vehicle-injected optic nerves. Shown are images representative of 4 optic nerves per group. Scale bar = 200 µm.

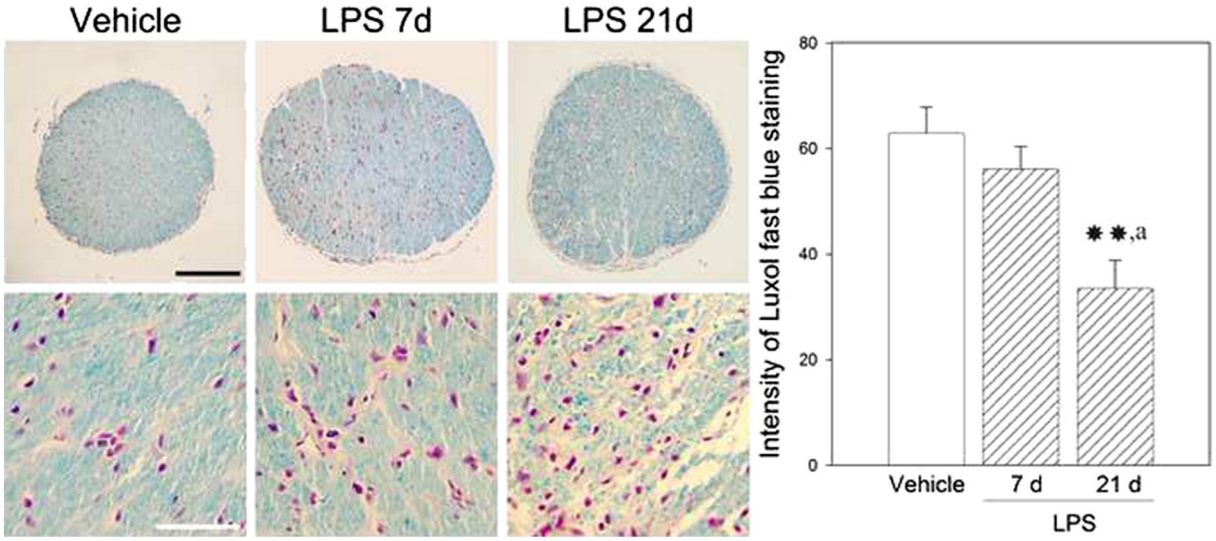

Fig. 8. Effect of LPS on optic nerve myelination. Representative cross-sections from optic nerves at 21 days post-injection of vehicle, and at 7, and 21 days post-injection of LPS, stained with luxol fast blue (details in the lower panel). A compact myelin staining was observed in vehicle- and LPS-injected optic nerves at 7 days post-injection. Note a less stained area in LPS-injected optic nerve at 21 days post-injection. Right panel: Evaluation of optic nerve demyelination by quantification of the intensity of the staining. LPS induced a significant demyelination of the optic nerve at 21 days post-injection. Data are mean ± SEM (n: 5 optic nerves/group). $^{**}P < 0.01$ *vs.* vehicle, a: $P < 0.05$ *vs.* LPS at 7 days post-injection, by Tukey's test. Black scale bar = 200 μm, white scale bar = 50 μm.

et al., 2000). Howell et al. (2010) have demonstrated that in MS and EAE, the disruption of the axon/oligodendrocyte association is involved in axonal damage and it occurs in parallel with local microglia activation. In contrast, the present results indicate that microglia/macrophages activation assessed by Iba-1 and ED1 immunohistochemistry, occurred as early as 1 day and 4 days post-injection of LPS, respectively, well ahead of axon-myelin structure alterations which were evident at 21 days post-injection, supporting that activation of microglia/macrophages may represent one of the earliest events in the neuroinflammatory disease induced by the injection of LPS into the optic nerve.

Although it has been shown that astrocyte responses contribute to EAE pathology (Brambilla et al., 2012), in LPS-injected optic nerves, the reactive gliosis assessed by GFAP-immunoreactivity was also a late event which occurred concomitantly with axonal and myelin alterations (shown by MBP-immunoreactivity and luxol fast blue staining). Besides their role in myelination, oligodendrocytes also support and promote the survival of neurons. Thus, disruption of their interaction could still contribute to axonal degeneration (reviewed by Morrison et al., 2013; Nave, 2010).

In the current study, ~50% of RGCs were lost in retinas whose optic nerves were injected with LPS, which is in agreement with results

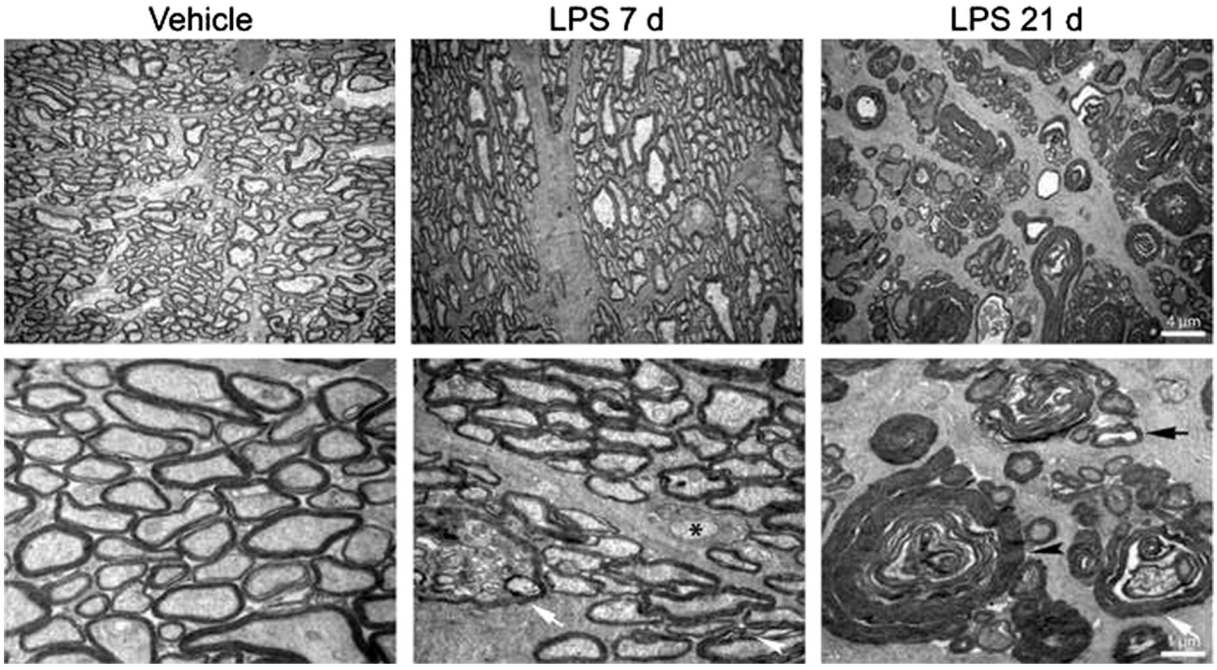

Fig. 9. Effect of LPS on optic nerve ultrastructure. Representative transversal sections from a vehicle-injected optic nerve (at 21 days post-injection), and from a LPS-injected optic nerve at 7 or 21 days post-injection. Note the presence of some degenerated axons (white arrow), unmyelinated axons (asterisk), and zones of unpacked myelin (white arrow head) at 7 days post-LPS. The presence of lamellar bodies (black arrow), lamellar bodies without axons (black arrow head), and degenerated axons was evident at 21 days post-injection of LPS. Shown are images representative of 4 optic nerves per group.

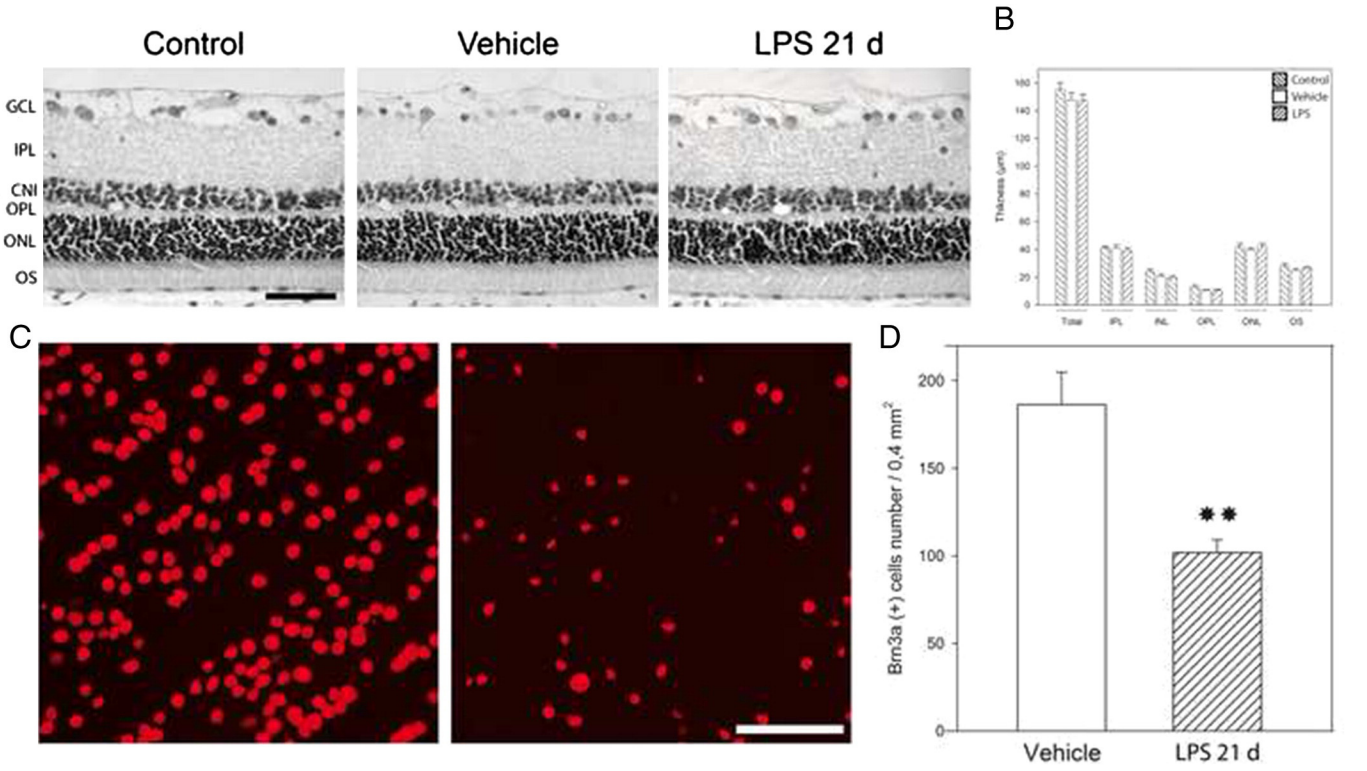

Fig. 10. Analysis of retinal structure and RGC number. Panel A: Representative photomicrographs of retinal sections from an eye whose optic nerve remained intact, or was injected with vehicle or LPS at 21 days post-treatment. No evident alterations in retinal morphologic features were observed. Panel B: Total retinal and retinal layer thicknesses in control, vehicle, and LPS groups. No significant differences in total retina, IPL, INL, OPL, ONL, and OS thickness were observed among groups. IPL, inner plexiform layer; INL, inner nuclear layer; OPL, outer plexiform layer; ONL, outer nuclear layer; OS, photoreceptor outer and inner segment. Panel C: Representative photomicrographs of Brn3a immunostaining in flat-mounted retinas whose optic nerve was injected with vehicle or LPS at 21 days post-treatment. Panel D: Quantification of Brn3a(+) cells. A significant decrease in the number of Brn3a(+) cells was observed in retinas whose optic nerves were injected with LPS at 21 days post-treatment. Data are the mean ± SEM (n = 5 retinas/group). $^{**}P < 0.01$ *vs.* vehicle, by Student's *t*-test. Black scale bar = 50 μm, white scale bar = 100 μm.

obtained by other groups using different strategies to induce autoimmune ON (Fairless et al., 2012; Khan et al., 2014; Maier et al., 2004; Shindler et al., 2006), and supports that ON induced by LPS is not merely an inflammatory condition, but it also involved a significant neurodegeneration. The delayed time course of RGC loss which was evident at 21 days post-injection of LPS is in contrast to that reported in relapsing EAE and in rats with chronic EAE. However, a similarly late time in RGC loss was described in C57/BL6 mice immunized with MOG (Quinn et al., 2011). Axonal damage often results in axonal degeneration and permanent loss of the cell body. Damaging the optic nerve by transection or crush, leads to a rapidly induced stress response in RGCs which finally results in neuron death (Quigley et al., 1995; Barron et al., 1986; You et al., 2012). Therefore, it seems likely that axonal damage could account for the RGC loss induced by LPS.

As shown herein, the timing of gliosis, demyelination, axonal degeneration, and RGC loss following the injection of LPS into the optic nerve, suggests that inflammation itself, resident cells of the CNS that have immune-inflammatory competence (*i.e.*, microglia), and infiltrating macrophages play an active role in demyelination and axonal injury that then leads to RGC loss. This observation is in line with the demonstration that RGC number was significantly lower in eyes with severe-massive optic nerve inflammation as compared to eyes with only mild-moderate inflammation in a transgenic model of autoimmune ON (Guan et al., 2006). In contrast to the current study, RGC loss in MOG-EAE rats occurs prior to detectable optic nerve inflammation (Hobom et al., 2004). However, it is possible that the MOG-EAE rats may develop early subclinical inflammation that is below the level of detection or, alternatively, that the early loss of RGCs detected in this model is induced by a direct effect of the MOG peptide, as it was suggested by Guan et al. (2006). Inflammation within the CNS is a common feature of neurological disorders and infection, but whether it contributes directly to neuronal or glial damage *in vivo* can be difficult to determine (Felts et al., 2005). The identification of mechanisms triggering neuronal death and injury is an intense area of research requiring reliable models. In this vein, the injection of LPS into the optic nerve would be a useful paradigm to identify underlying cellular and molecular mechanisms leading to inflammation-induced neuron loss. In this experimental model, systemic inflammation and cerebral involvement seems unlikely, as shown by the fact that LPS injection neither affected the body temperature, nor peripheral white blood cell and cerebrospinal fluid cell number. Experimental models of ON represent important tools in advancing our understanding and developing new therapies for the disease. The present results support that the injection of LPS directly into the optic nerve would constitute a new model of primary ON. Essentially because of the small size of the rat optic nerve, an intensive training was needed to optimize the injection procedure. However, after this training, we were able to obtain highly reproducible results at functional and histologic level. Another concern was the potential injury of the optic nerves by the needle insertion and injection-induced local pressure. However, in our experimental setting, the injection *per se* was innocuous, as shown by the fact that the functional and histological results did not differ between intact and vehicle-injected optic nerves. Although this new model differed from EAE- or lysolecithin-induced ON, it shares the common feature of recapitulating the inflammatory, demyelinating, and neurodegenerative components of this disorder.

Conclusions

Although care must be taken when extrapolating data obtained in experimental models to humans, these results suggest that in the primary form of ON, there would be a temporal window after patients

become symptomatic due to optic nerve inflammation and visual dysfunctions (VEPs and PLR), but before axonal, myelin, and somatic damage has occurred, in which therapies can be initiated to prevent permanent loss of axons and RGCs, which are recognized as the cellular events responsible for persistent visual deficit in patients with ON. Thus, this new model might pave the way for the identification of potential neuroprotective agents for primary ON treatment.

Supplementary data to this article can be found online at http://dx.doi.org/10.1016/j.expneurol.2015.01.010.

Acknowledgments

The authors wish to thank Dr. Esteban M. Reppeto for his help in peripheral white blood cell and cerebrospinal fluid cell number assessment. This research was supported by grants from the Agencia Nacional de Promoción Científica y Tecnológica [PICT 1623]; the University of Buenos Aires [20020100100678]; Consejo Nacional de Investigaciones Científicas y Técnicas [PIP 1911], Argentina. The funding organizations have no role in the design or conduct of this research. The authors report no conflicts of interest.

References

Barron, K.D., Dentinger, M.P., Krohel, G., Easton, S.K., Mankes, R., 1986. Qualitative and quantitative ultrastructural observations on retinal ganglion cell layer of rat after intraorbital optic nerve crush. J. Neurocytol. 15, 345–362.

Beck, R.W., Cleary, P.A., Anderson, M.M. Jr, Keltner, J.L., Shults, W.T., Kaufman, D.I., Buckley, E.G., Corbett, J.J., Kupersmith, M.J., Miller, N.R., Savino, P.J., Guy, J.R., Trobe, J.D., McCrary, J.A.I.I.I., Smith, C.H., Chrousos, G.A., Thompson, H.S., Katz, B.J., Brodsky, M.C., Goodwin, J.A., Atwell, C.W., the Optic Neuritis Study Group, 1992. A randomized, controlled trial of corticosteroids in the treatment of acute optic neuritis. N. Engl. J. Med. 326, 581–588.

Belforte, N., Sande, P.H., de Zavalía, N., Fernandez, D.C., Silberman, D.M., Chianelli, M.S., Rosenstein, R.E., 2011. Ischemic tolerance protects the rat retina from glaucomatous damage. PLoS ONE 6, e23763.

Bettelli, E., Pagany, M., Weiner, H., Linington, C., Sobel, R., Kuchroo, V., 2003. Myelin oligodendrocyte glycoprotein-specific T cell receptor transgenic mice develop spontaneous autoimmune optic neuritis. J. Exp. Med. 197, 1073–1081.

Blanc, F., Ballonzoli, L., Marcel, C., De, M.S., Jaulhac, B., De, S.J., 2010. Lyme optic neuritis. J. Neurol. Sci. 295, 117–119.

Bourdiol, F., Toulmond, S., Serrano, A., Benavides, J., Scatton, B., 1991. Increase in omega 3 (peripheral type benzodiazepine) binding sites in the rat cortex and striatum after local injection of interleukin-1, tumour necrosis factor-alpha and lipopolysaccharide. Brain Res. 543, 194–200.

Brambilla, R., Dvoriantchikova, G., Barakat, D., Ivanov, D., Bethea, J.R., Shestopalov, V.I., 2012. Transgenic inhibition of astroglial NF-κB protects from optic nerve damage and retinal ganglion cell loss in experimental optic neuritis. J. Neuroinflammation 9, 213.

Consiglio, A.R., Lucion, A.B., 2000. Technique for collecting cerebrospinal fluid in the cisterna magna of non-anesthetized rats. Brain Res. Brain Res. Protoc. 5, 109–114.

Constantino, T., Digre, K., Zimmerman, P., 2000. Neuro-ophthalmic complications of sarcoidosis. Semin. Neurol. 20, 123–137.

Costello, F., 2013. The afferent visual pathway: designing a structural–functional paradigm of multiple sclerosis. ISRN Neurol. 2013, 134858.

Costello, F., Coupland, S., Hodge, W., Lorello, G.R., Koroluk, J., Pan, Y.I., Freedman, M.S., Zackon, D.H., Kardon, R.H., 2006. Quantifying axonal loss after optic neuritiswith optical coherence tomography. Ann. Neurol. 59, 963–969.

Cunningham, C., 2013. Microglia and neurodegeneration: the role of systemic inflammation. Glia 61, 71–90.

de Seze, J., Arndt, C., Stojkovic, T., Ayachi, M., Gauvrit, J.Y., Bughin, M., Saint Michel, T., Pruvo, J.P., Hache, J.C., Vermersch, P., 2001. Pupillary disturbances in multiple sclerosis: correlation with MRI findings. J. Neurol. Sci. 188, 37–41.

Diem, R., Demmer, I., Boretius, S., Merkler, D., Schmelting, B., Williams, S.K., Sättler, M.B., Bähr, M., Michaelis, T., Frahm, J., Brück, W., Fuchs, E., 2008. Autoimmune optic neuritis in the common marmoset monkey: comparison of visual evoked potentials with MRI and histopathology. Invest. Ophthalmol. Vis. Sci. 49, 3707–3714.

Dorfman, D., Fernandez, D.C., Chianelli, M., Miranda, M., Aranda, M.L., Rosenstein, R.E., 2013. Post-ischemic environmental enrichment protects the retina from ischemic damage in adult rats. Exp. Neurol. 240, 146–156.

Eggenberger, E.R., 2001. Inflammatory optic neuropathies. Ophthalmol. Clin. North Am. 14, 73–82.

Ellis, C.J., 1979. The afferent pupillary defect in acute optic neuritis. J. Neurol. Neurosurg. Psychiatry 42, 1008–1017.

Fairless, R., Williams, S.K., Hoffmann, D.B., Stojic, A., Hochmeister, S., Schmitz, F., Storch, M.K., Diem, R., 2012. Preclinical retinal neurodegeneration in a model of multiple sclerosis. J. Neurosci. 32, 5585–5597.

Felekis, T., Katsanos, K., Kitsanou, M., Trakos, N., Theopistos, V., Christodoulou, D., Asproudis, I., Tsianos, E.V., 2009. Spectrum and frequency of ophthalmologic manifestations in patients with inflammatory bowel disease: a prospective single-center study. Inflamm. Bowel Dis. 15, 29–34.

Felts, P.A., Woolston, A.M., Fernando, H.B., Asquith, S., Gregson, N.A., Mizzi, O.J., Smith, K.J., 2005. Inflammation and primary demyelination induced by the intraspinal injection of lipopolysaccharide. Brain 128, 1649–1666.

Fernandez, D.C., Sande, P.H., de Zavalía, N., Belforte, N., Dorfman, D., Casiraghi, L.P., Golombek, D., Rosenstein, R.E., 2013. Effect of experimental diabetic retinopathy on the non-image-forming visual system. Chronobiol. Int. 30, 583–597.

Frigui, M., Frikha, F., Sellemi, D., Chouayakh, F., Feki, J., Bahloul, Z., 2011. Optic neuropathy as a presenting feature of systemic lupus erythematosus: two case reports and literature review. Lupus 20, 1214–1218.

Furlan, R., Cuomo, C., Martino, G., 2009. Animal models of multiple sclerosis. Methods Mol. Biol. 549, 157–173.

Gamlin, P.D., 2006. The pretectum: connections and oculomotor-related roles. Prog. Brain Res. 151, 379–405.

Guan, Y., Shindler, K.S., Tabuela, P., Rostami, A.M., 2006. Retinal ganglion cell damage induced by spontaneous autoimmune optic neuritis in MOG-specific TCR transgenic mice. J. Neuroimmunol. 178, 40–48.

Halliday, A., McDonald, W., Mushin, J., 1972. Delayed visual evoked response in optic neuritis. Lancet 1, 982–985.

Herrera, A.J., Castaño, A., Venero, J.L., Cano, J., Machado, A., 2000. The single intranigral injection of LPS as a new model for studying the selective effects of inflammatory reactions on dopaminergic system. Neurobiol. Dis. 7, 429–447.

Hickman, S.J., Dalton, C.M., Miller, D.H., Plant, G.T., 2002. Management of acute optic neuritis. Lancet 360, 1953–1962.

Hobom, M., Storch, M.K., Weissert, R., Maier, K., Radhakrishnan, A., Kramer, B., Bähr, M., Diem, R., 2004. Mechanisms and time course of neuronal degeneration in experimental autoimmune encephalomyelitis. Brain Pathol. 14, 148–157.

Hood, D., Odel, J., Zhang, X., 2000. Tracking the recovery of local optic nerve function after optic neuritis: a multifocal VEP study. Invest. Ophthalmol. Vis. Sci. 41, 4032–4038.

Horstmann, L., Schmid, H., Heinen, A.P., Kurschus, F.C., Dick, H.B., Joachim, S.C., 2013. Inflammatory demyelination induces glia alterations and ganglion cell loss in the retina of an experimental autoimmune encephalomyelitis model. J. Neuroinflammation 10, 120.

Horwitz, H., Friis, T., Modvig, S., Roed, H., Tsakiri, A., Laursen, B., Frederiksen, J.L., 2014. Differential diagnoses to MS: experiences from an optic neuritis clinic. J. Neurol. 261, 98–105.

Howell, O.W., Rundle, J.L., Garg, A., Komada, M., Brophy, P.J., Reynolds, R., 2010. Activated microglia mediate axoglial disruption that contributes to axonal injury in multiple sclerosis. J. Neuropathol. Exp. Neurol. 69, 1017–1033.

Kallenbach, K., Frederiksen, J.L., 2008. Unilateral optic neuritis as the presenting symptom of human immunodeficiency virus toxoplasmosis infection. Acta Ophthalmol. 86, 459–460.

Kaufman, D.I., Trobe, J.D., Eggenberger, E.R., Whitaker, J.N., 2000. Practice parameter: the role of corticosteroids in the management of acute monosymptomatic optic neuritis. Report of the Quality Standards Subcommittee of the American Academy of Neurology. Neurology 54, 2039–2044.

Khan, R.S., Dine, K., Luna, E., Ahlem, C., Shindler, K.S., 2014. HE3286 reduces axonal loss and preserves retinal ganglion cell function in experimental optic neuritis. Invest. Ophthalmol. Vis. Sci. 55, 5744–5751.

Klistorner, A., Arvind, H., Nguyen, T., Garrick, R., Paine, M., Graham, S., O'Day, J., Grigg, J., Billson, F., Yiannikas, C., 2008. Axonal loss and myelin in early ON loss in post acute optic neuritis. Ann. Neurol. 64, 325–331.

Kondo, Y., Takada, M., Honda, Y., Mizuno, N., 1993. Bilateral projections of single retinal ganglion cells to the lateral geniculate nuclei and superior colliculi in the albino rat. Brain Res. 608, 204–215.

Kupersmith, M.J., Nelson, J.I., Seiple, W.H., Carr, R.E., Weiss, P.A., 1983. The 20/20 eye in multiple sclerosis. Neurology 33, 1015–1020.

Lachapelle, F., Bachelin, C., Moissonnier, P., Nait-Oumesmar, B., Hidalgo, A., Fontaine, D., Baron-Van Evercooren, A., 2005. Failure of remyelination in the nonhuman primate optic nerve. Brain Pathol. 15, 198–207.

Lin, T.H., Kim, J.H., Perez-Torres, C., Chiang, C.W., Trinkaus, K., Cross, A.H., Song, S.K., 2014. Axonal transport rate decreased at the onset of optic neuritis in EAE mice. Neuroimage 100C, 244–253.

Maier, K., Rau, C.R., Storch, M.K., Sättler, M.B., Demmer, I., Weissert, R., Taheri, N., Kuhnert, A.V., Bähr, M., Diem, R., 2004. Ciliary neurotrophic factor protects retinal ganglion cells from secondary cell death during acute autoimmune optic neuritis in rats. Brain Pathol. 14, 378–387.

Martínez-Lapiscina, E.H., Fraga-Pumar, E., Pastor, X., Gómez, M., Conesa, A., Lozano-Rubí, R., Sánchez-Dalmau, B., Alonso, A., Villoslada, P., 2014. Is the incidence of optic neuritis rising? Evidence from an epidemiological study in Barcelona (Spain), 2008–2012. J. Neurol. 261, 759–767.

Matsunaga, Y., Kezuka, T., An, X., Fujita, K., Matsuyama, N., Matsuda, R., Usui, Y., Yamakawa, N., Kuroda, M., Goto, H., 2012. Visual functional and histopathological correlation in experimental autoimmune optic neuritis. Invest. Ophthalmol. Vis. Sci. 53, 6964–6971.

Moro, S.I., Rodriguez-Carmona, M.L., Frost, E.C., Plant, G.T., Barbur, J.L., 2007. Recovery of vision and pupil responses in optic neuritis and multiple sclerosis. Ophthalmic Physiol. Opt. 27, 451–460.

Morrison, B.M., Lee, Y., Rothstein, J.D., 2013. Oligodendroglia: metabolic supporters of axons. Trends Cell Biol. 23, 644–651.

Nave, K.A., 2010. Myelination and support of axonal integrity by glia. Nature 468, 244–252.

Optic Neuritis Study Group, 2008. Multiple sclerosis risk after optic neuritis: final optic neuritis treatment trial follow-up. Arch. Neurol. 65, 727–732.

Perry, V.H., Teeling, J., 2013. Microglia and macrophages of the central nervous system: the contribution of microglia priming and systemic inflammation to chronic neurodegeneration. Semin. Immunopathol. 35, 601–612.

Quigley, H.A., Nickells, R.W., Kerrigan, L.A., Pease, M.E., Thibault, D.J., Zack, D.J., 1995. Retinal ganglion cell death in experimental glaucoma and after axotomy occurs by apoptosis. Invest. Ophthalmol. Vis. Sci. 36, 774–786.
Quinn, T.A., Dutt, M., Shindler, K.S., 2011. Optic neuritis and retinal ganglion cell loss in a chronic murine model of multiple sclerosis. Front. Neurol. 2, 50.
Rangachari, M., Kuchroo, V.K., 2013. Using EAE to better understand principles of immune function and autoimmune pathology. J. Autoimmun. 45, 31–39.
Salido, E.M., Dorfman, D., Bordone, M., Chianelli, M., González Fleitas, M.F., Rosenstein, R.E., 2013. Global and ocular hypothermic preconditioning protect the rat retina from ischemic damage. PLoS ONE 8 (4), e61656.
Shindler, K.S., Guan, Y., Ventura, E., Bennett, J., Rostami, A., 2006. Retinal ganglion cell loss induced by acute optic neuritis in a relapsing model of multiple sclerosis. Mult. Scler. 12, 526–532.
Shindler, K.S., Revere, K., Dutt, M., Ying, G.S., Chung, D.C., 2012. In vivo detection of experimental optic neuritis by pupillometry. Exp. Eye Res. 100, 1–6.
Simmons, S.B., Pierson, E.R., Lee, S.Y., Goverman, J.M., 2013. Modeling the heterogeneity of multiple sclerosis in animals. Trends Immunol. 34, 410–422.
Toosy, A.T., Mason, D.F., Miller, D.H., 2014. Optic neuritis. Lancet Neurol. 13, 83–99.
Trip, S.A., Schlottmann, P.G., Jones, S.J., Altmann, D.R., Garway-Heath, D.F., Thompson, A.J., Plant, G.T., Miller, D.H., 2005. Retinal nerve fiber layer axonal loss and visual dysfunction in optic neuritis. Ann. Neurol. 58, 383–391.
Wilejto, M., Shroff, M., Buncic, J.R., Kennedy, J., Goia, C., Banwell, B., 2006. The clinical features, MRI findings, and outcome of optic neuritis in children. Neurology 67, 258–262.
You, Y., Klistorner, A., Thie, J., Graham, S.L., 2011. Latency delay of visual evoked potential is a real measurement of demyelination in a rat model of optic neuritis. Invest. Ophthalmol. Vis. Sci. 52, 6911–6918.
You, Y., Gupta, V.K., Graham, S.L., Klistorner, A., 2012. Anterograde degeneration along the visual pathway after optic nerve injury. PLoS ONE 7, e52061.
Zhu, B., Moore, G.R., Zwimpfer, T.J., Kastrukoff, L.F., Dyer, J.K., Steeves, J.D., Paty, D.W., Cynader, M.S., 1999. Axonal cytoskeleton changes in experimental optic neuritis. Brain Res. 824, 204–217.